AUTOMATIC NON PARAMETRIC PROCEDURES FOR TERRESTRIAL LASER POINT CLOUDS PROCESSING

Alberto Beinat, Fabio Crosilla, Domenico Visintini, Francesco Sepic

Department of Georesources & Territory, University of Udine, via Cotonificio, 114 I-33100 Udine, Italy
alberto.beinat@uniud.it; fabio.crosilla@uniud.it; domenico.visintini@uniud.it; sepic@dimi.uniud.it

KEY WORDS: Laser scanning, detection, registration, segmentation, classification.

ABSTRACT
The paper deals with the registration and modelling of terrestrial laser point clouds. For both problems a non parametric regression is suitably exploited, whose unknowns are the function values and the partial derivatives of a second order Taylor's expansion estimated for a certain number of surface points. These allow to directly estimate local curvatures, namely *Gaussian*, *mean* and *principal* values. Relating to the registration problem, tie points are automatically detected from point clusters having extreme *Gaussian* curvature values. The centroids of such clusters generate a vertexes configuration: the point to point correspondences are automatically defined by the analysis of the respective adjacency matrices. For these sets of pairs, the pre-alignment roto-translation parameters are computed by a SVD algorithm, while the final alignment is executed by an ICP method. The paper further proposes a method to directly detect the discontinuities (segmentation) and to successively estimate the parameters for each recognized surface (classification). For both goals, the algorithm exploits again the curvature values: the discontinuity contours are characterized by points having *mean* curvature greater than a threshold, while classification is performed by a cluster analysis of points having homogeneous curvature values. Some numerical examples show the proper applicability of the proposed method for coarse and fine registration of different scans, for edge detection, and for surface primitives classification.

1. INTRODUCTION

As well-known registration, segmentation and classification are three main phases of laser data processing once different point clouds are available for a certain object. To automatically carry out these phases in a sequential way, a non parametric analytical technique is proposed in this paper (section 2).
About the registration, a hybrid technique, to automatically execute the alignment of close range point clouds by evidencing their morphological singularities, is presented (section 3). The method is developed by studying the local *Gaussian* curvature values, computed from the partial derivatives of the Taylor's expansion, by running a clustering procedure of points having extreme curvature values, and finally by determining the centroids of each cluster. For every point cloud, the centroids generate a vertexes configuration. Once the centroids set of pairs are identified, the pre-alignment roto-translation is estimated by a SVD algorithm. The refined alignment is completed by a variant of the ICP method.
In order to reconstruct the geometric primitives embedded in the point cloud, the paper further proposes a method to directly detect the discontinuities (segmentation) and to successively estimate the surface primitives of each recognized object (classification). For both aims, the algorithm exploits the local curvature parameters. Slope discontinuities of the surfaces are evidenced by studying the values of the *mean* curvature (section 4). The procedure allows to automatically identify the band of points corresponding to such edges, since characterised by mean curvature values greater than a fixed threshold.
Within each volumetric primitive, a region growing method is accomplished (section 5). Points belonging to the same feature model are characterised, first, by a strict correspondence among the measured height values and the estimated ones, second, for plane surfaces, by a constant value of the first order partial derivatives, and third, for curvilinear surfaces, by a constant value of the *Gaussian* and *mean* curvatures. Finally a *forward search* procedure allows a robust and refined classification of the remaining points belonging to the studied primitives.
Some numerical examples show the proper applicability of the proposed method with simulated and real noisy data (section 6).

2. APPLICATION OF A NON PARAMETRIC REGRESSION MODEL

As already mentioned, the fundamental steps of the cloud registration and the shape reconstruction mainly exploit the same analytical model based on a nonparametric regression. The main advantage of this approach consists in its full generality, since it does not require any a priori knowledge of the point geometry or the analytical function of interpolation.

2.1. Estimation of local surface parameters

Let us consider the following polynomial model of second order terms (Cazals and Pouget, 2003):

$$Z_j = a_0 + a_1 u + a_2 v + a_3 u^2 + a_4 uv + a_5 v^2 + \varepsilon_j \qquad (1)$$

where the coefficients and the parameters are locally related to a measured value Z_j by a Taylor's expansion of the function $Z = \mu + \varepsilon$ in a neighbour point *i* of *j*, as:

$$a_0 = Z_{0_i}; \quad a_1 = \left(\frac{\partial Z}{\partial X}\right)_{X_i}; \quad a_2 = \left(\frac{\partial Z}{\partial Y}\right)_{Y_i}; \quad a_3 = \frac{1}{2}\left(\frac{\partial^2 Z}{\partial X^2}\right)_{X_i};$$

$$a_4 = \left(\frac{\partial^2 Z}{\partial X \partial Y}\right)_{X_i, Y_i}; \quad a_5 = \frac{1}{2}\left(\frac{\partial^2 Z}{\partial Y^2}\right)_{Y_i}; \quad u = (X_j - X_i); \quad v = (Y_j - Y_i)$$

with X_i, Y_i and X_j, Y_j plane coordinates of points *i* and *j*.
The parameters a_i $(i \neq 0)$ are the first and second order partial derivatives along X,Y directions in the *i*-th point of the best interpolating local surface, collected in the vector:

$$\boldsymbol{\beta} = \begin{bmatrix} a_0 & a_1 & a_2 & a_3 & a_4 & a_5 \end{bmatrix}^T$$

where a_0 is the estimated function value at point *i*.

The weighted least squares estimate of the unknown vector $\boldsymbol{\beta}$ from a limited number of *p* neighbour points results as:

$$\hat{\boldsymbol{\beta}} = (\mathbf{X}^T\mathbf{Q}\mathbf{X})^{-1}\mathbf{X}^T\mathbf{Q}\mathbf{z} \qquad (2)$$

where (for j = 1, …, p):

- **X** is the coefficient matrix, with *p* rows as:

$$\mathbf{X}_j = \begin{bmatrix} 1 & u & v & u^2 & uv & v^2 \end{bmatrix}$$

- **Q** is a diagonal weight matrix defined by a symmetric kernel function centred at the *i*-th point, with diagonal elements as:

$$w_{ij} = \left[1-(d_{ij}/b)^3\right]^3 \text{ for } d_{ij}/b<1 \quad w_{ij}=0 \text{ for } d_{ij}/b\geq 1$$

where d_{ij} is the distance between the points *i*,*j* and *b* is the half radius of the window encompassing the *p* closest points to *i*. The value of *b*, rather than the kernel function, is critical for the quality in estimating $\boldsymbol{\beta}$. In fact, the greater is the value of *b*, the smoother the regression function results, while the smaller is the value of *b*, the larger is the variance of the estimated value.

As last remark, to apply the second order Taylor expansion (1), the coordinate Z must be univocally defined by X,Y coordinates. This is always true for aerial laser data, where the laser strips are all aligned and geo-referenced e.g. in E,N,H coordinates, while for terrestrial data the scans geometry is more complex. Each point cloud has a different local X,Y,Z reference system, the scans can be panoramic in azimuthal plane and, for some laser devices, quasi-panoramic in the zenithal plane, i.e. with points in the entire direction sphere. To avoid ambiguous cases, it is thus necessary to share the cloud in more sub-clouds. Moreover, it could be necessary a permutation among X,Y,Z coordinates in order to assume, as Z-axis for (1), the direction whose Z values results better expressed as function of the X,Y ones. In other words, points displaced onto quasi "vertical" surfaces are not well modelled by expansion (1).

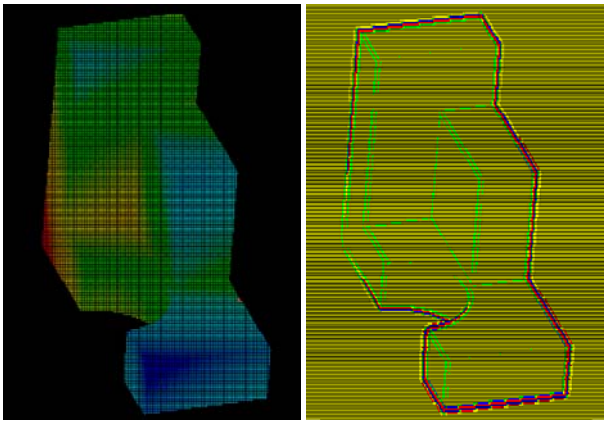

Figure 1: Simulated laser points of the *curvblock-1* model coloured by Z_i values (at left) and by $Z_i - Z_{0_i}$ (at right).

Figure 1 reports the simulated scan *curvblock-1* as example throughout the paper: it comes from the OSU Range Image database (Ohio State University) and has been also experimented by Alshawabkeh, Haala and Fritsch (2006). In Figure 1 at left, the points are coloured by the original Z_i values, since no coordinate permutation is required. At right, the same points are coloured by $Z_i - Z_{0_i}$ absolute values, explainable as the smoothing effect of the regressive interpolation: the external edges of the object clearly appear, while the internal ones are not significantly recognised.

2.2 Computation of local curvatures values

For the local analysis of a surface *S* obtained from a point cloud, a great support is provided by geometric quantities coming from differential geometry, in particular by local *Gaussian, mean* and *principal* curvatures values. These ones can be obtained from the so-called "*Weingarten map*" matrix **A** of the surface *S* (e.g. Do Carmo, 1976), that is given by:

$$\mathbf{A} = -\begin{bmatrix} e & f \\ f & g \end{bmatrix}\begin{bmatrix} E & F \\ F & G \end{bmatrix}^{-1} \qquad (3)$$

where E, F, and G are the coefficients of the so-called "*first fundamental form*", obtained from the parameters estimated by (2) as follows:

$$E = 1+a_1^2; \quad F = a_1 a_2; \quad G = 1+a_3^2$$

e, f, and g are the "*second fundamental form*" coefficients, as:

$$e = 2a_3\Big/\sqrt{a_1^2+1+a_2^2}; \quad f = a_4\Big/\sqrt{a_1^2+1+a_2^2}; \quad g = 2a_5\Big/\sqrt{a_1^2+1+a_2^2}$$

The *Gaussian* curvature K corresponds to the determinant of **A**:

$$K = \frac{eg-f^2}{EG-F^2} \qquad (4)$$

The *mean* curvature H can be instead obtained from:

$$H = \frac{eG-2fF+gE}{2(EG-F^2)} \qquad (5)$$

The *principal* curvatures k_{max} and k_{min}, corresponding to the eigenvalues of **A**, are given instead from the solution of the system $k^2-2Hk+K=0$, i.e. from $k_{min,max} = H \pm \sqrt{H^2-K}$.

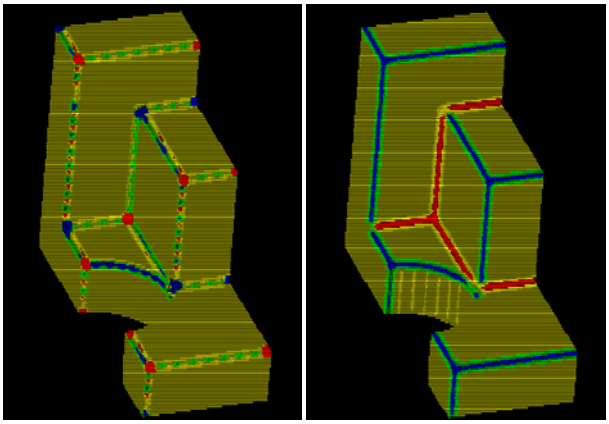

Figure 2: Points coloured by K (at left) and by H values (at right).

Further usable relationships for the curvature values are: $K = k_{min}k_{max}$ and $H = (k_{min}+k_{max})/2$.

It is interesting to observe in Figure 2 how, thanks to the different geometrical meaning, the *Gaussian* curvature K (at left) can be mainly exploited for the point clouds registration, while the *mean* curvature H (at right) for the edge detection.

Summarizing, for each *i*-th laser point, four local curvature

values K, H, k_{max} and k_{min} can be automatically obtained as functions of the vector $\boldsymbol{\beta}$ terms. Furthermore, such curvatures are invariant to the reference frame rotations, providing a very important property in analyzing the surface shape.

3. POINT CLOUDS REGISTRATION

3.1 Vertexes detection by means of the K curvature values

Once the *Gaussian* curvature K values are determined by (4) for all the sampled points, it is worthwhile to consider those having extreme absolute values, represented in Figure 2 at left with blue and red dots: they are the "vertexes" of the scanned object. Such points, automatically detected, can be exploited as "tie points" for registration purposes. More properly, since clusters of points with extreme K values will be found, the mean of their 3D coordinates (the centroid) is considered. The set of thus determined centroids constitutes the first point configuration to submit to a correspondence search. This process is repeated for all the clouds that have to be registered, defining in this way a series of centroid configurations.

3.2 Automatic feature matching and labelling

The centroids identified at step 3.1 form a set of possible candidates to be homologous points of adjacent clouds. The next step consists in the recognition of topological relationships existing among the clusters (labelling problem).
Let us consider two partially overlapped point clouds, from which two sets **p** and **q**, respectively constituted by *m* and *n* tie points, have been individuated, as represented in Figure 3.
The problem consists in defining the intersection **p**∩**q,** and in automatically finding out, within the intersection, the probable correspondences between the tie points of the sets **p** and **q.**

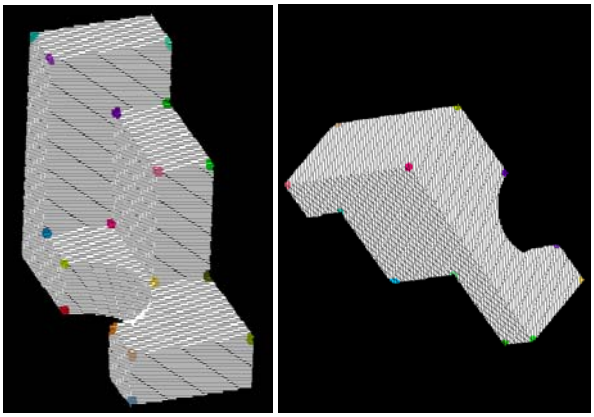

Figure 3: Vertexes detected for *curvblock-1* and *curvblock-2*.

First of all, we assume that no scale variation exists between the coordinate systems of **p** and **q**. This simplified hypothesis is correct according to the purpose of this operation. The implemented method runs in the following way:

1. Let us consider $\mathbf{p} = \{p_1 \dots p_m\}$ the arbitrary *m* points configuration. The *m*×*m* symmetric adjacency matrix $\mathbf{D}^p$ of this configuration contains among its terms the Euclidean distance $d^p_{i,j} = \|p_i - p_j\|$ between points p_i and p_j.
2. In the same way, for the arbitrary n points configuration $\mathbf{q} = \{q_1 \dots q_n\}$, the *n*×*n* adjacency matrix $\mathbf{D}^q$ is defined.
3. The row of maximal asymmetry $\mathbf{d}^p_{i\,max}$ is searched in $\mathbf{D}^p$ (or in $\mathbf{D}^q$), whose distinct elements, ordered in terms of magnitude, present the "maximal minimal difference", i.e.: $\mathbf{d}^p_{i\,max} := \left\{ d^p_{i,j} \geq d^p_{i,j+1};\ \max_{i=1\dots m}\left[\min_{i,j=1\dots m-1} \left(d^p_{i,j} - d^p_{i,j+1} \right) \right] \in \mathbf{d}^p_{i\,max} \right\}$. This search minimizes the possibility of ambiguous geometrical configurations.
4. In the row $\mathbf{d}^p_{i\,max}$ of maximal asymmetry, the greatest element $d^p_{i,j\,max} = \max\left[\mathbf{d}^p_{i\,max}\right]$ is identified. Next step consists in searching $d^p_{k,l} := \left\{ \left| d^p_{i,j\,max} - d^p_{k,l} \right| \leq \varepsilon; \forall k, \forall l < k \right\}$ in $\mathbf{D}^q$, where ε is a prefixed tolerance. The satisfying values *k*,*l* are stored into a pointer array, i.e. the list of the possible pairs (q_k, q_l) corresponding to $(p_i, p_j)_{max}$. If this set is empty, the search is repeated considering the next component to $d^p_{i,j\,max}$ in terms of magnitude.
5. The various pairs of possible correspondences (q_k, q_l) are orderly considered. For each row of $\mathbf{D}^q$, where one of the correspondence pairs is present, the equivalence of the remaining elements of the same row with respect to the possible elements of $\mathbf{d}^p_{i\,max}$, within a fixed tolerance, is verified. This allows to generate a binary table, of size *m*×*n*, where the elements express the possible correspondence among the points of **p** and of **q**, according to the initial choice for *i* max and *k*, respectively.
6. If this table has at least two not null elements, a cross-validation of all the possible correspondences is carried out. This is performed verifying the equivalence among all the remaining distances defined by point pairs of **p** and analogous point pairs of **q**, inserted into the table.
7. This process is repeated for each pair (q_k, q_l) identified at sub-step 4, adopting the pair generating the largest number of valid correspondences between **p** and **q**.

A set of implemented tests, makes it possible to solve ambiguous situations. In the next version, to evaluate the correspondence point degree, some attributes associable to the points (e.g. curvatures), will be employed.

3.3 SVD pre-registration

Thanks to the pairs of tie points, identified and related by steps 3.1 and 3.2, two matrices of corresponding point coordinates are obtained. Translations and rotations (without the scale factor), to transform the coordinates of a point cloud onto another one, are determined by applying the SVD method.

3.4 Registration refinement by ICP

Once the pre-registration is obtained, the process is completed by ICP. In our case, a basic version of the method proposed by Besl and Mc Kay (1992) has been implemented, updated by some variants proposed in the literature.

The procedure is here described in the essential way, referring to Beinat, Crosilla and Sepic (2006) for the details.
In performing the registration of three *curvblock* scans, after the detection 3.1 of the tie points reported in Figure 3, the point matching 3.2, the pre-registration 3.3, and the refined registration 3.4 have provided a global model with a very good congruence. It is represented in Figure 4, where *curvblock-1* is coloured in blue, *curvblock-2* in green, and *curvblock-4* in red.

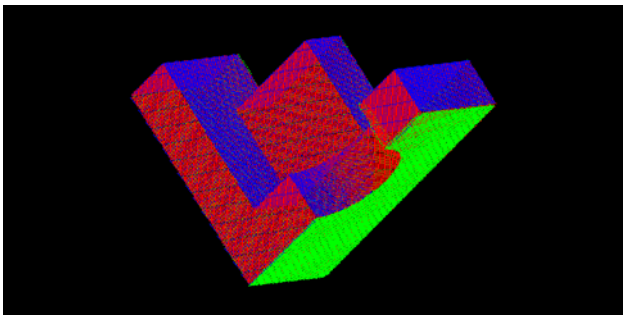

Figure 4: Resulting *curvblock* from a three clouds registration.

4. POINT CLOUD EDGE DETECTION

Once the laser points have been merged into a unique cloud, the incoming problem is the extrapolation of the geometric shape of the surveyed objects with the maximum level of automation. This topic represents the main challenge dealing with the laser scanning technique, namely the maintenance in the data processing of the extraordinary automation level of the data acquisition. In this sense, the different expressions used in literature as edge detection, object recognition, shape classification, and surface reconstruction can be considered as complementary approaches of the same more general problem, defined as "automatic interpretation" of the laser data. This is not a trivial topic and the difficulty grows if we consider noisy mid-long range laser data rather than precise close range ones. In addition, scenes as typical in architectural surveying are more complex than in the industrial environments, since lots of single objects or irregular surfaces occur.

4.1 Edge detection problems: kinds of discontinuity

From the mathematical point of view, the discontinuities of a $Z = f(X, Y)$ surface can be as follows:

D0: Step discontinuity: the Z values of a significant number of points displaced along a certain X,Y direction present a jump (i.e. the C0 continuity is not fulfilled);

D1: Slope discontinuity: the inclination values of a C0 surface change locally (C1 continuity is not satisfied);

D2: Curvature discontinuity: one of the principal curvatures of a C1 surface changes locally (C2 continuity is not granted).

The difficulty in detecting such discontinuities increases with the rank, anyway the term "edge detection" is mainly thought as the D1 slope discontinuities search. Furthermore, dealing with objects surveyed from a lot of scan positions, the happening of D0 discontinuities normally disappear.

4.2 Analytical and geometrical methods of edge detection

From the methodological point of view, the edge detection problem can be carried out by (at least) three methods, classified as "analytical direct", "analytical indirect" and "geometrical by decimation".

The algorithms involving surface interpolations by any analytical function belong to the first class. These have the common property to provide one or more local numerical values directly revealing singularities in the laser cloud. Interesting models have been proposed by the research groups of the Technical University of Wien (Briese, 2006) and the University of Stuttgart (Alshawabkeh, Haala and Fritsch, 2006). The methods belonging to the second family deal instead, first of all, with the suitable estimation of continuous surfaces better interpolating the laser cloud. Only in a second step, the D1 and D2 edges are detected by considering the space intersection of such surfaces or simply analyzing to which surface each point has been assigned. An analytical procedure proposed by the authors for the classification and the segmentation of laser data (Crosilla, Visintini and Sepic, 2005, 2007) belongs to this class.

As general consideration about direct or indirect methods, their most critical characteristics are the requirement of high quality laser data, falling down the efficiency in presence of noisy data, and the modeling complication when a large numbers of parameters have to be estimated.

With a geometric approach, implemented in many commercial software of solid modelling, a TIN mesh is engaged. In this way, the numerical processes applied, as the smoothing and the decimation, regards the optimization of the mesh and does not involve the coordinate points; so this method can be defined as "geometrical". For this reason, the D1 edge detection is not thus a straight goal of this approach, anyway the edges are strongly correlated with the result of a process of vertex decimation: in fact, they well correspond to the so-called "feature edges" of the triangles remaining after the decimation. Interesting methods are reported in computer vision literature (e.g. Garland, 1997).

As reported before, the analytical indirect method proposed, allows detecting the surface primitives from an undistinguished laser cloud. It proceeds in the four following steps:

1. Estimation of a local surface by a non parametric Taylor's expansion (as seen in subsection 2.1);
2. Computation of *Gaussian* K, *mean* H and *principal* k_{max} and k_{min} local curvatures (as reported in subsection 2.2);
3. Raw segmentation of the cloud in homogeneous clusters by a region-growing method considering also curvature values;
4. Refined segmentation of the raw clusters by a robust parametric regression for each cluster, so estimating the parameters of the various interpolating surfaces.

Focusing the attention to the detection of the three kinds of discontinuity, the following strategy is proposed:

- D0 edges: by checking if the $Z_i - Z_{0_i}$ absolute value is greater than a fixed threshold, as seen in Figure 1 at right.
- D1 edges: by evaluating if the H absolute value is greater than a fixed threshold; the threshold value, as for D0, is fixed considering the noise and the density of the data.
- D2 edges: by estimating the surfaces and by considering the sign and the values variation of K and H.

Nevertheless, the points detected in the previous way must be geometrically significant, that is a certain number of points displaced within a small buffer volume lengthened in one direction should be found. Furthermore, to transform such points in a vector 3D polyline, a suitable chaining or a space interpolation has to be applied.

A rearrangement of the four steps method is now proposed. To detect D1 edges, one more analysis is performed after the second step (see subsection 4.3). In this way, the procedure becomes a direct method of edge detection. Steps 3. and 4. are instead carried out to detect D2 edges, since these curvature discontinuities are found in indirect mode by applying a robust parametric model (see section 5): thanks to this approach, the reliability of the achieved detection should be satisfactory.

4.3 D1 detection by means of the H curvature values

The attention is now focused onto the estimated values of the local *mean* curvature H. The analysis of H values, proposed by the Stuttgart School (Alshawabkeh, Haala and Fritsch, 2006) exploits the property that such index is closely related to the first variation (slope) of a surface area that locally well reveals

possible D1 edges. Since H is the average of k_{max} and k_{min}, it is numerically slightly less sensitive to the noise with respect to K curvature, which is instead the product of k_{max} and k_{min}. Extreme absolute values of H are therefore searched: this point buffer volume so reveals the D1 edges we are looking for.

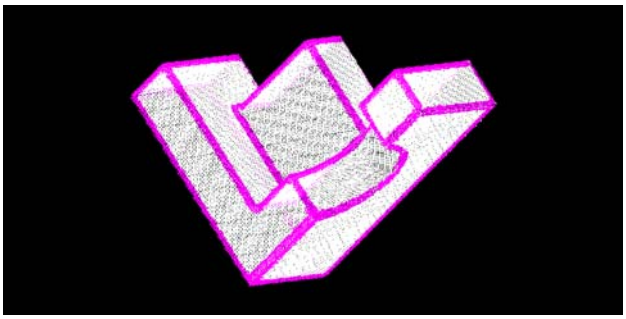

Figure 5: Extreme values H corresponding to possible edges.

This criterion has been implemented in a routine that paints by pink colour the points with H absolute value greater than a threshold, so evidencing the D1 edge zones, as in Figure 5.

5. SURFACE SEGMENTATION AND CLASSIFICATION

As mentioned before, D2 edges are the most difficult elements to automatically detected, especially with noisy data. To this aim and when the main interest of the surveyor is anyway about the overall surface rather than its local discontinuities, efficient methods for its segmentation and classification assume the main importance in the whole flow-chart of data processing.

5.1. Raw surface segmentation by a region-growing method

Analyzing the sign and the values of K and H, a preliminary clustering of the whole cloud is made possible. Each surface can be classified into one of the following basic types (see Table 6): hyperbolic ($K < 0$), parabolic ($K = 0$ but $H \neq 0$), planar ($K = H = 0$), and elliptic ($K > 0$).

	K < 0 : **hyperbolic**	K = 0 : **parabolic/planar**	K > 0 : **elliptic**
H < 0	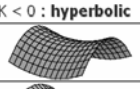	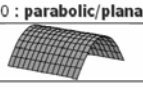	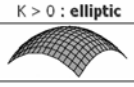
H = 0	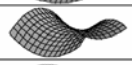	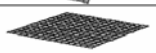	not possible
H > 0		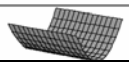	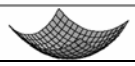

Table 6. Classification of surfaces according to the values of *Gaussian* K and *mean* H curvatures (from Haala et al., 2004).

This allows to classify the various volumetric primitives and to define a priori the polynomial degree of the parametric model to apply for the refined segmentation (step 5.2).
Hence, to classify and segment the dataset, a region growing method is applied, starting from a random point not yet belonging to any subset. The surrounding points having a distance less than the bandwidth *b* are analysed, by evaluating the values of the estimated height Z_{0_i} and the values of K and H. If the neighbour points present difference values within a threshold, fixed according to the noise level, then they are labelled as belonging to the same class and putted into a list. The same algorithm is repeated for each list element, till this is fully completed. Afterwards, the procedure restarts again from a new random point, ending when every point has been analysed.
Summarising, a first raw segmentation of the whole dataset is carried out in this way: hence, each cluster represents an initial subset to submit to the next refining segmentation step 5.2.

5.2. Refined surface segmentation by a parametric model

Previous authors papers report in detail this step (Crosilla, Visintini and Sepic, 2005, 2007): it is based on the application of a Simultaneous AutoRegressive (SAR) model to describe the trend surface of each point cluster, and on an iterative *Forward Search* (FS) algorithm (Cerioli and Riani, 2003) to find out outliers. Starting from a cluster detected as in step 5.1, the FS approach allows a robust estimation of the SAR unknown parameters. At each iteration, one or more points are joined according to their agreement with the surface model. If some statistical diagnostics reveal an incoming outlier, the growing process is interrupted: the surface is so bounded, hence a refined segmentation is achieved.
Figure 7 shows for *curvblock* point cloud the correct result of the classification, that is one cylinder face (K=0, H>0), twelve planes (K=0, H=0), and the refined segmentation of the model.

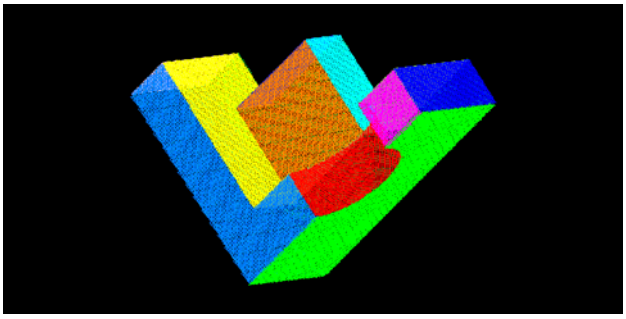

Figure 7: Classification and refined segmentation of the different surfaces: cylinder in red, plane faces in other colours.

6. NUMERICAL EXPERIMENTS

The numerical testing of the proposed procedures has been carried out with satisfactory results for the *curvblock* model scans and for other synthetic objects of the OSU Range Image database. Only some brief comments about the two models depicted in Figure 8 are reported in this paper.

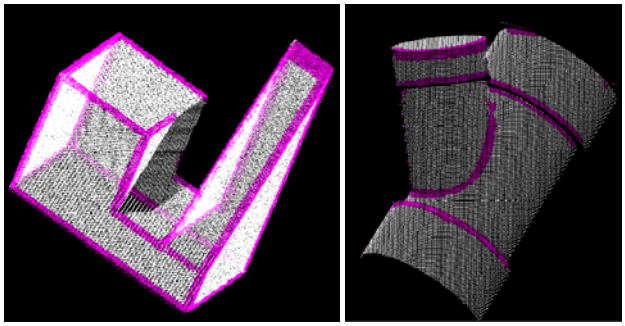

Figure 8: D1 Edges detected for *block2* and for *bigwye* model

The *block2* model (at left) has been joined by registering five partial clouds, exploiting its various vertexes detected by K values analysis. The global point cloud results correctly registered, anyway a central part without points remains for the incompleteness of the data, so yielding a D0 discontinuity. The detection of D1 edges by evaluating H values is completely fulfilled and, since all the surfaces are planes, steps 5.1 and 5.2 have not been carried out.
Model *bigwye* (at right) is instead constituted by curved surfaces: the D1 detection has been correctly accomplished as well as the classification 5.1 as cylinders with values $H < 0$.
Last but not least, to test the method in noisy conditions, some experiments have been performed onto real data acquired with a

Riegl Z360i laser system onto the façade of the baroque Church of Saint Ignatius in Gorizia (Italy). Figure 9 evidences, within more than 500.000 laser points, those having extreme K values, well corresponding to vertexes of the architectonic elements of the façade, and exploitable for registration purposes.

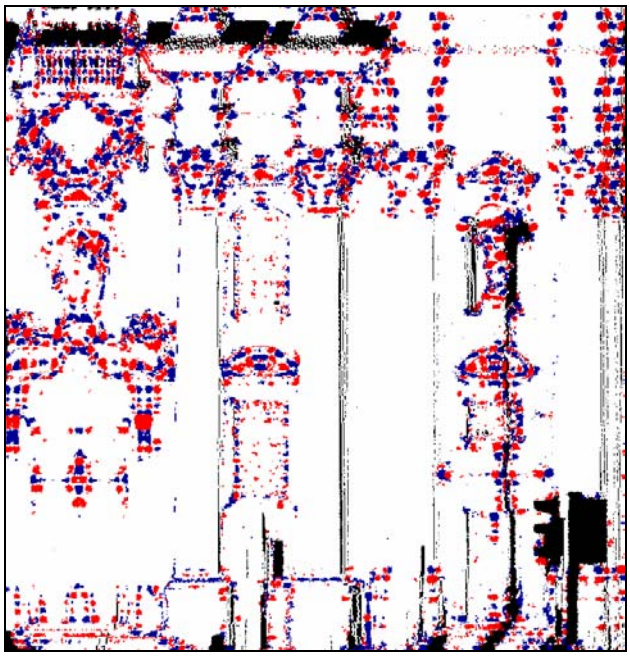

Figure 9: Real points with extreme K values (blue < 0, red > 0).

Figure 10 shows instead the points with extreme H values, well congruent with the vertical and horizontal edges of the façade.

Figure 10: Real points with extreme H values (blue < 0, red > 0).

The results of this D1 edge detection appear quite satisfactory, particularly in comparison with those geometrically achieved by commercial software implementing TIN decimation tools.

7. CONCLUSIONS

The paper reports a sequential non parametric procedure, mainly based on local estimation of second order Taylor's expansion partial derivatives, to automatically perform registration, segmentation and classification of laser clouds.
The estimated curvature values allow the automatic detection of singularities in the clouds: registration tie points are evidenced by analyzing the local *Gaussian* curvatures, while segmentation edge points result by evaluating the *mean* curvatures.
The obtained results, for synthetic and real noisy laser data, emphasize the capability of the method proposed for the processing of terrestrial laser surveys.

REFERENCES

Alshawabkeh, Y., Haala, N., Fritsch, D., 2006. 2D-3D feature extraction and registration of real world scenes, in: *IAPRS&SIS*, XXXVI, 5, Dresden, 32-37.

Beinat, A., Crosilla, F., Sepic, F., 2006. Automatic morphological pre-alignment and global hybrid registration of close range images, in: *IAPRS&SIS*, XXXVI, 5, Dresden (on CD).

Besl, P. J., McKay, N. D., 1992. A method for registration of 3-D shapes, *IEEE Transactions on Pattern Analysis and Machine Intelligence*, 14, 239-256.

Briese, C., 2006, Structure line modelling based on terrestrial laser scanner data, in: *IAPRS&SIS*, XXXVI, 5, Dresden (on CD).

Cazals, F., Pouget, M., 2003. Estimating differential quantities using polynomial fitting of osculating jets. in: *Proceedings of the 1st Symposium on Geometry Processing*, 177-187.

Cerioli, A., Riani, M., 2003. Robust methods for the analysis of spatially autocorrelated data. *Statistical Methods & Applications*, 11, 334-358.

Crosilla, F., Visintini, D., Sepic, F., 2005. A segmentation procedure of LIDAR data by applying mixed parametric and nonparametric models, in: *IAPRS&SIS*, XXXVI, 3/W19, Enschede, 132-137.

Crosilla, F., Visintini, D., Sepic, F., 2007. An automatic classification and robust segmentation procedure of spatial objects. *Statistical Methods & Applications*, 15, 329-341.

Do Carmo, M.P., 1976. *Differential geometry of curves and surfaces*, Prentice-Hill International, London.

Garland, M., 1999. Multiresolution modeling: Survey & future opportunities", *Eurographics '99*, State of the Art Report, Sept.

Haala, N.; Reulke, R.; Thies, M.; Aschoff, T., 2004. Combination of terrestrial laser scanning with high resolution panoramic images for investigations in forest applications and tree species recognition, in: *IAPRS&SIS*, XXXIV, 5/W16, Dresden.

Ohio State University: *OSU MSU/WSU Range Image Database*, http://sampl.ece.ohio-state.edu/data/3DDB/RID/index.htm

ACKNOWLEDGEMENTS

This work was carried out within the research activities supported by the INTERREG IIIA Italy-Slovenia 2003-2006 project "Cadastral map updating and regional technical map integration for the GIS of the regional agencies by testing advanced and innovative survey techniques".
The authors thank Francesco Crosilla for providing some analytical computations at the beginning of the research.